PHYSICOCHEMICAL CHARACTERIZATION OF IONICALLY CROSS-LINKED HYDROGEL MATRICES WITH INCORPORATED FANANSERIN DERIVATIVE

Sandra Komaniecka[1]*, Kacper Odziomek[1], Przemysław Zaręba[2], Katarzyna Bialik-Wąs[3]*

[1] Cracow University of Technology,
Faculty of Chemical Engineering and Technology,
24 Warszawska St., 31-155 Cracow, Poland
[2] Cracow University of Technology,
Faculty of Chemical Engineering and Technology,
Department of Chemical Technology
and Environmental Analytics,
24 Warszawska St., 31-155 Cracow, Poland
[3] Cracow University of Technology,
Faculty of Chemical Engineering and Technology,
Department of Chemistry and Technology of Polymers,
24 Warszawska St., 31-155 Cracow, Poland
*e-mail: sandra.komaniecka@student.pk.edu.pl,
katarzyna.bialik-was@pk.edu.pl

Abstract

The fananserin derivative, such as 1-{6-[4-(2-fluorophenyl)piperazin-1-yl]hexyl}-benzo[cd]indol-2(1H)-one (compound FL-4), represents an interesting biologically active substance that can be incorporated into polymeric carriers. Due to its highly hydrophobic nature and poor solubility in conventional solvents, FL-4 was incorporated into a delivery system to improve its solubility, stability, and bioavailability. Based on preliminary studies and DLS analysis, an optimal concentration of FL-4 (10 mg) was selected, ensuring system stability. This system was incorporated into polymer matrices, resulting in two hydrogel delivery systems: M10-J, containing FL-4, and M10-T-J, which combines a thermosensitive nanocarrier with FL-4, both ionically cross-linked. The systems were evaluated for their physicochemical properties, including swelling abilities, degradation, chemical structure (based on FTIR spectra analysis), morphology (based on SEM images), and substance release profiles. The M10-T-J samples showed a swelling ratio of 0.27 g/g in PBS and 0.35 g/g in water, while M10-J exhibited 0.16 g/g in PBS and 0.2 g/g in water. The pH and conductivity analysis suggested a faster degradation process for M10-T-J hydrogel compared to M10-J. FT-IR analysis confirmed the chemical structure of the materials, revealing significant changes in M10-T-J samples, indicating interactions between FL-4 and $CaCl_2$ used during cross-linking. SEM and EDS analysis showed a uniform distribution of FL-4 on the matrix surface in both hydrogel variants, with the addition of the thermosensitive nanocarrier not significantly affecting the morphology. The M10-J hydrogel exhibited rapid release of FL-4 within the first 4 h, while M10-T-J showed limited release.

Keywords: *drug delivery system, fananserin derivative, hydrogel, thermoresponsive nanocarrier, transdermal systems*

[Engineering of Biomaterials 173 (2025) 05]

doi:10.34821/eng.biomat.173.2025.05

Submitted: 2025-04-15, Accepted: 2025-05-20, Published: 2025-05-23

Introduction

Fungal and bacterial infections pose a significant threat to public health, particularly among people with weakened immune systems. High-risk groups include, among others, HIV-positive individuals, organ transplant recipients, and patients suffering from diabetes, liver, kidney, or respiratory diseases, as well as other comorbid conditions. Any disturbances in immune function and imbalances in the microbiota contribute to the development of opportunistic infections [1-3].

Cryptococcus neoformans is a mycopathogen that presents a serious risk for immunocompromised patients, causing, among other conditions, cutaneous cryptococcosis. Without effective treatment, this infection can lead to severe, life-threatening complications such as cryptococcal meningitis or sepsis [4-6].

The compound FL-4 (1-{6-[4-(2-fluorophenyl)piperazin-1-yl]hexyl}-benzo[cd]indol-2(1H)), initially developed as a potential antidepressant, has also shown antimicrobial activity, particularly against *C. neoformans*. Notably, the activity of this compound has also been observed against other pathogens such as *Candida albicans*, responsible for fungal infections, and *Escherichia coli*, a bacterium causing urinary and gastrointestinal tract infections. Its broad-spectrum activity makes it a promising therapeutic option for the treatment of various infections [7-9].

Given the highly hydrophobic nature of the FL-4 compound and its poor solubility in aqueous environments and conventional solvents, its direct therapeutic application is significantly limited. Therefore, this study aimed to design, synthesize, and comprehensively characterize FL-4-loaded hydrogel-based and thermoresponsive polymeric delivery systems, to improve the compound's solubility, stability, and controlled release properties, while preserving its antimicrobial activity under physiological conditions [10,11].

Hydrogels are polymer-based materials capable of absorbing water up to several hundred or even several thousand percent of their dry weight, depending on the degree of cross-linking, due to the presence of a three-dimensional polymer network that gives them gel-like properties. Due to their high water content and elasticity, they closely resemble human tissues, making them biocompatible [12-14]. Their structure allows for effective encapsulation of active substances, particularly hydrophilic compounds, while also protecting them from harmful external factors, such as pH fluctuations, temperature, or humidity. One of the most critical steps in hydrogel synthesis is the selection of polymers capable of forming a three-dimensional network, which ensures mechanical stability and resistance to external forces [14-17].

Particular attention has been given to hydrogels formed via ionic cross-linking, which does not require chemical initiators. The resulting materials are generally non-toxic and biocompatible; however, their lower mechanical stability limits them to short-term applications, such as wound dressings [18,19]. Ionic cross-linking involves the formation of bonds between polymers and divalent metal ions (e.g., Ca^{2+}, Mg^{2+}, Fe^{2+}). One of the most commonly used polymers for this purpose is sodium alginate, which, in the presence of calcium ions, forms the characteristic "egg-box" structure [20-23].

Another important class of carriers includes thermoresponsive polymers, also known as intelligent carriers. These polymers exhibit a sol-gel transition at temperatures close to physiological body temperature (approx. 36°C), enabling controlled drug release and enhancing both stability and biological efficacy. Owing to their ability to respond to natural physiological temperature changes, these polymers have gained widespread application in both *in vitro* and *in vivo* studies [24-29].

Materials and Methods

N-Isopropylacrylamide (CAS 2210-25-5) and N,N'-methylenebisacrylamide (CAS 110-26-9) from Sigma-Aldrich (Saint Louis, MO, USA), along with gum arabic (CAS 05.01.9000) from POCH S.A. (Gliwice, Poland), were used for synthesizing thermosensitive polymeric nanocarriers, with ammonium persulfate (CAS 7727-54-0) from POCH S.A. serving as a reaction initiator. Hydrogel preparation utilized sodium alginate (CAS 9005-38-3) from Sigma-Aldrich, *Aloe vera* lyophilizate (CAS 85507-69-3) from Zrób sobie krem (Prochowice, Poland), calcium chloride (CAS 10035-04-8) from POCH S.A., and propylene glycol (CAS 57-55-6) from Chempur (Piekary Śląskie, Poland). The active substance, fananserin derivative (FL-4) was provided by the Department of Chemical Technology and Environmental Analytics. Additional reagents included: methanol (96%, v/v; CAS 67-56-1) and ethyl alcohol (96%, v/v; CAS 64-17-5) from Chempur, buffer solutions (pH 7.4; CAS 7778-77-0) from Chempur.

Synthesis of the thermosensitive polymer nanocarrier

The thermosensitive nanosystem was obtained through the emulsion polymerization of N-isopropylacrylamide (0.2% w/v) and N,N'-methylenebisacrylamide (0.002% w/v) in a 0.5% w/v solution of arabic gum. The mixture was heated to 70°C in a glycerin bath under an inert gas atmosphere, then the initiator (APS 0.025% w/v) was added and the mixture was heated at 80°C for 4 h. After the reaction was complete, the thermosensitive nanosystem was purified using cellulose membranes (MWCO = 14,000 Da) for 7 days [30-31].

Encapsulation of fananserin derivative in thermosensitive nanocarrier

The encapsulation process began by adding 10 mg of FL-4 compound, dissolved in methyl alcohol, to 2.5 mL of the purified thermosensitive nanocarrier. The mixture was placed in a round-bottom flask and vigorously stirred at a speed of 1200 rpm for 3 h at room temperature. After the process was complete, the FL-4 compound–thermosensitive nanocarrier system was frozen and then lyophilized [32-34].

Preparation of hydrogel carriers with directly incorporated fananserin derivative via ionic cross-linking

For the synthesis of hydrogels obtained by ionic cross-linking, a 3% (w/v) sodium alginate solution and a 3% (w/v) aloe solution were prepared and mixed on a magnetic stirrer for 1 h at a constant speed of 800 rpm. The solutions were then combined in a 1:1 volume ratio, ensuring a final volume of 30 ml. During intensive mixing (1200 rpm), 10 mg of FL-4 compound, previously dissolved in propylene glycol (1.7% v/v) using ultrasound, was added. After 10 min, the mixture was transferred to a Petri dish, left for 15 min, and then covered with a 5% (w/v) calcium chloride solution. After another 15 minutes, the $CaCl_2$ solution was poured off from the Petri dish. The resulting hydrogel was then rinsed with distilled water, and the excess surface water was gently removed by lightly touching the hydrogel with filter paper. The final product was an ionically cross-linked hydrogel containing the FL-4 compound [22,35].

Preparation of hydrogel carriers containing the FL-4-thermosensitive nanocarrier system

The synthesis of hydrogels containing a dual delivery system of FL-4 compound, based on a thermosensitive nanocarrier, follows the previously described method. The procedure remains almost identical, with the difference that instead of the compound alone dissolved in propylene glycol, the lyophilized FL-4–thermosensitive nanocarrier system, also previously dissolved in the same solvent using ultrasound, is added.

Dynamic light scattering (DLS)

To determine the average particle size of the obtained thermosensitive nanocarrier and in the systems containing the FL-4 compound, a Zetasizer Nano ZS (Malvern, United Kingdom) was used. Measurements were made at 25°C using disposable polystyrene cuvettes.

Determination of swelling degree

To determine the swelling ratio (SR%), samples of the obtained hydrogel carriers were prepared and immersed in excess distilled water and phosphate buffered saline (PBS, pH = 7.4). The samples were weighed before immersion (W_0) and then placed in immersion fluids. After specified time intervals, that is, 1, 2, and 24 h, the swollen samples were gently dried with filter paper and reweighed (W_t). The water absorption for all the tested samples was determined based on the following equation (1):

$$\%SR = (W_t - W_0)/W_0 \cdot 100\% \quad (1)$$

Degradation studies

For each hydrogel sample, 200 ± 5 mg was weighed and placed in 30 ml of distilled water or PBS. The pH and electrical conductivity were then measured at specified time intervals for each sample. The studies were conducted over 23 days at room temperature.

Attenuated total reflectance Fourier transform infrared spectroscopy (ATR-FTIR)

To determine the chemical structure of the tested polymer carriers and to compare the hydrogel matrices with the FL-4–thermosensitive nanocarrier system, FT-IR spectrum analysis was performed. Studies were conducted using a Thermo Scientific Nicolet iS5 FT-IR spectrometer equipped with an iD7 ATR accessory, in the transmission range of 4000–400 cm^{-1}.

Scanning electron microscopy with energy dispersive X-ray spectroscopy (SEM+EDS)

Morphological analysis was performed using a scanning electron microscope (SEM), equipped with an energy dispersive X-ray spectroscopy (EDS) system, using the Apreo 2 S LoVac scanning electron microscope (Thermo Fisher Scientific, Waltham, MA, USA), with an UltraDry EDS detector and Octane Elect (EDAX Ametek GmbH, Weiterstadt, Germany). Before analysis, the tested hydrogels were immersed in excess distilled water for 1 h, then frozen for 24 h, and finally subjected to lyophilization to better visualize the pores in their structure. The prepared samples were coated with a thin layer of gold using a sputtering method and then analyzed for 90 s.

Studies on the release of FL-4 from the obtained carriers (static method)

Studies were conducted on the release of the FL-4 compound from the thermosensitive nanocarrier and hydrogel carriers using the static method. Initially, the mass of the entire hydrogel matrix was precisely determined. Then, four samples weighing 250 ± 5 mg were prepared and placed in dialysis membranes made of regenerated cellulose (Spectra/Por® MWCO 6000–8000 Da, Carl Roth®, Karlsruhe, Germany). The membranes with the samples were immersed in a thermostated chamber filled with 250 ml of PBS solution at pH 7.40 containing 1.5% (w/w) methanol. The mixing was performed at a constant temperature of 37°C, ensuring a uniform speed. At regular time intervals, 2 ml of fluid were taken from the chamber, and the volume loss was replenished with fresh acceptor medium.

Statistical analysis

The results of the dynamic light scattering and swelling ratio are expressed as mean ± standard deviation (SD) based on three independent experiments. Statistical comparisons between group means were performed using one-way ANOVA in Statistica Version 12 (StatSoft, Cracow, Poland).

Results and Discussions

DLS analysis of the thermoresponsive nanocarrier–compound FL-4 system

The average particle size of the unloaded thermoresponsive nanocarrier is approximately 118 nm [30]. The study began with the selection of a compound concentration that would maintain system stability. Various concentrations of compound FL-4 (10–50 mg) were introduced into the system. Stability was observed only for the sample containing 10 mg of FL-4, which exhibited an average particle size of approximately 233.4 ± 0.9 nm and a polydispersity index (PDI) of 0.352 ± 0.006. Samples containing 20 mg of the compound reached an average size of 1330 ± 10.4 nm and were characterized by high polydispersity (PDI = 0.527 ± 0.009) (TABLE 1). One-way ANOVA confirmed that raising the FL-4 dose from 10 mg to 20 mg caused a highly significant increase in both average particle size and polydispersity (Z-Average: $p = 5.3 \times 10^{-9}$; PDI: $p = 6.2 \times 10^{-6}$). Higher concentrations of the compound led to agglomeration, preventing reliable DLS analysis.

Despite the increase in average particle size following compound incorporation, the thermoresponsive nanocarrier system containing 10 mg of FL-4 remained the most stable, with no signs of aggregation. The increase in particle size results from the embedding of FL-4 molecules within the carrier structure; however, this process does not negatively affect the quality or properties of the obtained systems.

TABLE 1. Z-Average particle size and PDI for systems consisting of thermosensitive polymer nanocarrier and compound FL-4 in amounts of 10 and 20 mg (N-T-10 and N-T-20). Results are presented as mean values (n = 3).

Sample	Z-Average (d. nm)	Polydispersity index (PDI)
N-T-10	233.4 ± 0.9	0.352 ± 0.006
N-T-20	1330 ± 10.4	0.527 ± 0.009

Physicochemical analysis

Swelling ratio

The swelling ratio of the obtained hydrogel carriers containing the compound FL-4 is presented in FIG. 1.

The conducted study evaluated the swelling capacity of hydrogel carriers containing the compound FL-4, obtained in two variants: M10-J and M10-T-J. The differences in swelling degree between these systems arise not only from the applied method of compound incorporation but also from interactions among the system components, such as hydrophobic, electrostatic, and hydrogen bonding interactions.

In the M10-J hydrogels, where the compound FL-4 was introduced directly, the presence of calcium ions intensifies electrostatic and coordination interactions with the functional groups of FL-4. These interactions lead to the densification of the hydrogel structure by tightening the polymer network, thereby reducing the available space for water absorption. As a result, the swelling degree after 24 h ranges from 0.160 ± 0.005 to 0.220 ± 0.008 g/g. Interestingly, although ionically cross-linked hydrogels typically show higher swelling values (FIG. 1c), an opposite trend was observed in this case. This may be attributed to the strong interactions between FL-4 and calcium ions, which disturb the chemical structure of the systems and reduce their absorption capacity. In addition, after 24 h, the unloaded matrix swelled to 0.67 ± 0.006 g/g in water and 0.41 ± 0.008 g/g in PBS, i.e., markedly higher than any FL-4-loaded system. This confirms that introducing the drug either directly (M10-J) or via the nanocarrier (M10-T-J), densifies the polymer network and limits free-water uptake. Therefore, the M0 samples serve as an upper reference for the sorption capacity of the given polymer composition and highlight the trade-off between drug loading and hydrogel porosity.

In contrast, the M10-T-J variant, which utilizes a thermoresponsive nanocarrier system with compound FL-4, displays a modified distribution of FL-4 and weaker interactions between the components, resulting in the formation of a more spacious hydrogel matrix. Despite being ionically cross-linked, which is generally associated with lower porosity and a higher initial water content, the altered system characteristics allow for better medium absorption. This leads to a higher maximum swelling degree of 0.27 ± 0.007 – 0.35 ± 0.01 g/g after 24 h, which may be advantageous for applications requiring increased absorbency.

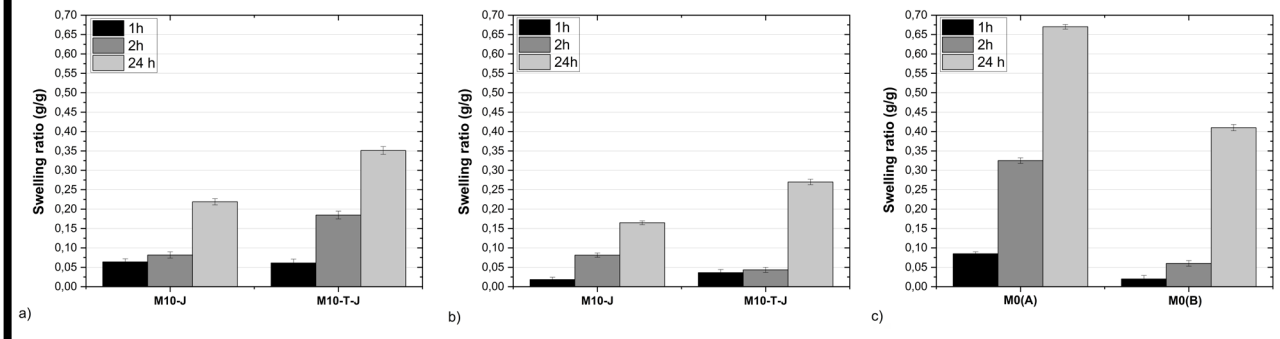

FIG. 1. Swelling ratio (g/g) of hydrogel carriers containing compound FL-4 (M10-J) and the thermoresponsive nanocarrier–compound FL-4 system (M10-T-J), ionically cross-linked; measured at room temperature after incubation in (a) distilled water and (b) PBS; and (c) the swelling ratio (g/g) of base hydrogel carriers ionically cross-linked; measured at room temperature after incubation in (M0(A)) distilled water and (M0(B)) PBS; (n = 3).

Moreover, the test environment significantly influenced the swelling behaviour of the hydrogels. The swelling degree in distilled water (FIG. 1a) was slightly higher than in PBS (FIG. 1b). This difference results from the presence of ions in the PBS solution, primarily phosphate ($H_2PO_4^-$, HPO_4^{2-}), as well as sodium (Na^+) and chloride (Cl^-) ions, which restrict the hydrogels' ability to absorb water by forming ionic interactions with the functional groups of the polymers, thus decreasing their capacity for free water uptake. In both environments, the swelling degree increased over time, reaching maximum values after 24 h. One-way ANOVA demonstrated a highly significant difference in the 24-h swelling ratios across the four conditions ($p = 1.1 \times 10^{-8}$).

Degradation studies

Degradation studies were carried out to assess the physicochemical stability of the obtained hydrogel carriers containing the FL-4 compound under different conditions: neutral and physiological. The results are presented in FIGs 2 and 3.

The initial pH values of the distilled water varied depending on the system. The hydrogel containing the thermoresponsive nanocarrier (M10-T-J) exhibited an initial pH of approximately 6.0, whereas the ionically cross-linked hydrogel without the nanocarrier (M10-J) showed a lower pH of approximately 5.25. In phosphate buffered saline (PBS), all samples showed similar initial pH values of around 7.85, consistent with the properties of the buffer environment.

In distilled water (FIG. 2a), a gradual increase in pH was observed in the hydrogel samples over the first seven days of incubation. Additionally, ion exchange processes and the gradual release of basic residues from within the polymer network may also contribute to the alkalization of the medium. After about 10 days, pH values in both hydrogel variants stabilized in the range of 6.8–6.9, suggesting the stabilization of the system's chemical composition.

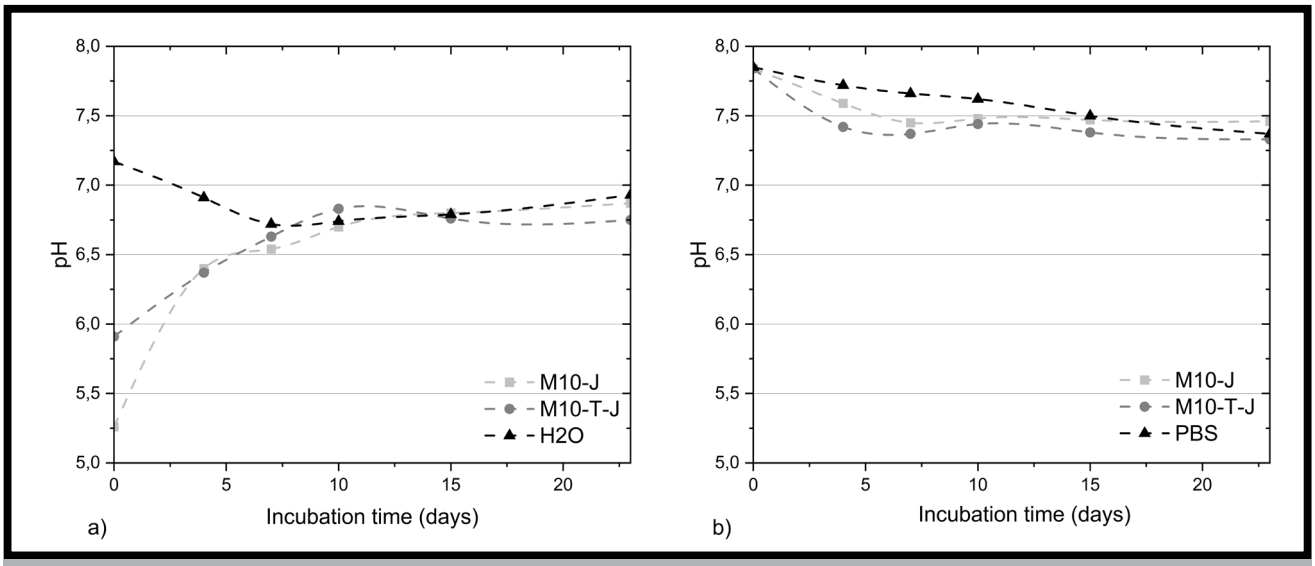

FIG. 2. Changes in pH values of the analyzed fluids: (a) distilled water and (b) PBS containing incubated hydrogel carrier samples with compound FL-4 (M10-J) and with the thermoresponsive nanocarrier–compound FL-4 system (M10-T-J) (room temperature).

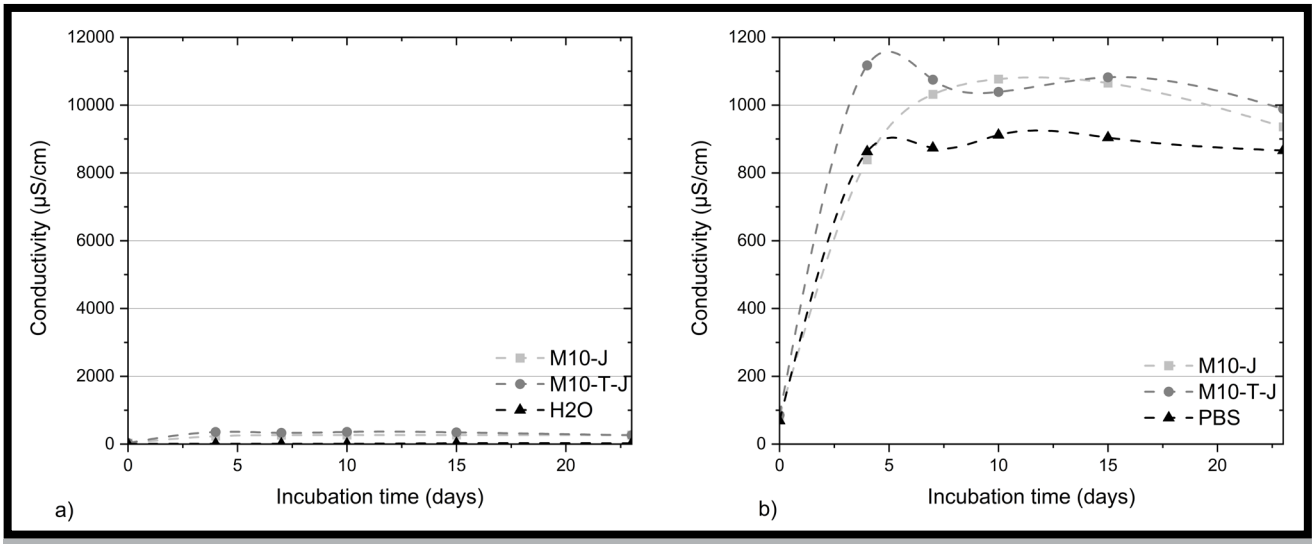

FIG. 3. Changes in conductivity of the analyzed fluids: (a) distilled water and (b) PBS containing incubated samples of hydrogel carriers with compound FL-4 (M10-J) and the thermoresponsive nanocarrier-compound FL-4 system (M10-T-J) (room temperature).

In PBS (FIG. 2b), a slight initial decrease in pH was recorded, likely resulting from interactions between the buffer and the hydrogel material. The M10-J variant reached a stable pH after 10 days of incubation, whereas in the case of M10-T-J, the stabilization process was significantly prolonged and only completed after 23 days. Final pH values were 7.46 for M10-J and 7.33 for M10-T-J, respectively.

The observed differences indicate that the presence of a thermoresponsive nanocarrier in the M10-T-J system negatively affected pH stability, most likely through interactions with the cross-linking agent ($CaCl_2$), which reduced the efficiency of forming stable ionic bonds. This phenomenon correlates with previous observations related to swelling, where the M10-T-J hydrogel exhibited higher water absorption compared to M10-J. These interactions may have disrupted the network structure, affecting both the dynamics of pH stabilization and the physicochemical properties of the material.

Additionally, the incorporation of the compound FL-4 may have contributed to the observed changes in pH and system stability. Due to its hydrophobic nature and complex chemical structure, FL-4 may interfere with the ionic cross-linking process by partially limiting the availability of functional groups on the polymer chains for interaction with divalent calcium ions. This effect can lead to a less compact or irregular polymeric network, which may be more susceptible to environmental factors such as ion exchange or hydrolysis. Moreover, the gradual release of FL-4 from the hydrogel matrix during incubation can alter the local ionic environment, particularly in the initial stages, when the release is more dynamic. The compound's interaction with the polymer or the cross-linking agent might also contribute to the prolonged pH stabilization process observed in the M10-T-J samples. These findings are consistent with structural and release studies, suggesting that both the carrier composition and the drug itself play a significant role in shaping the chemical stability and behaviour of the hydrogel systems.

Furthermore, the differences in pH behaviour observed in distilled water and PBS may also reflect partial degradation of the hydrogel matrix, which appeared more pronounced in the M10-T-J system. The reduced cross-linking efficiency, resulting from both the presence of the thermoresponsive nanocarrier and the incorporation of FL-4, likely contributed to the increased sensitivity of the hydrogel network to external conditions. Consequently, the material may have been more prone to structural disruption and gradual chemical degradation, leading to observable shifts in the pH of the surrounding medium.

In the distilled water environment (FIG. 3a), the initial conductivity for all analyzed samples was low (around 0–50 µS/cm), which is consistent with the minimal ion content in this medium. Over the first four days of incubation, a significant increase in conductivity was observed, reaching maximum values of 232 µS/cm for M10-J and 358 µS/cm for M10-T-J hydrogels. This phenomenon can be attributed to the gradual release of ions from the hydrogel matrix, including unreacted reagent residues (e.g., Ca^{2+}), as well as products of degradation processes or leaching of low-molecular-weight impurities present in the structure. The conductivity stabilized in the M10-J system after about 7 days, whereas in the M10-T-J sample, it took until 23 days of incubation (both 263 µS/cm), which is consistent with the pH stabilization observations and suggests longer-lasting processes of reorganization and ion exchange in the presence of the nanocarrier.

In PBS solution (FIG. 3b), the initial conductivity values were significantly higher due to the presence of ions in the phosphate buffer; after 4 days, they were around 865 µS/cm for M10-J and 1065 µS/cm for M10-T-J. Conductivity increased slightly and then stabilized after about 7 days for both hydrogel variants (within the range of 936–989 µS/cm).

The observed differences in the dynamics of conductivity changes suggest that the M10-T-J hydrogels are more susceptible to ion leaching, which may be due to disruptions in the ionic network structure caused by the presence of the thermoresponsive nanocarrier. On the other hand, the slower and less intense release of ions in the M10-J hydrogel may indicate a more compact and stable network system. These results confirm that the cross-linking method and the presence of additional components, such as the nanocarrier, significantly influence the conductivity of the hydrogel system, and thus its behaviour in both aqueous and buffered environments.

Structural analysis

The chemical structure of the obtained hydrogel carriers containing the compound FL-4 was confirmed based on FT-IR spectrum analysis (FIG. 4).

The FT-IR spectra of the examined hydrogel carriers (M10-J, M10-T-J) revealed the presence of the bands typical of functional groups of sodium alginate and *Aloe vera*. The band around ~3300 cm^{-1} corresponds to the stretching vibrations of the hydroxyl groups (-OH), confirming the presence of water residues in the matrix from the components.

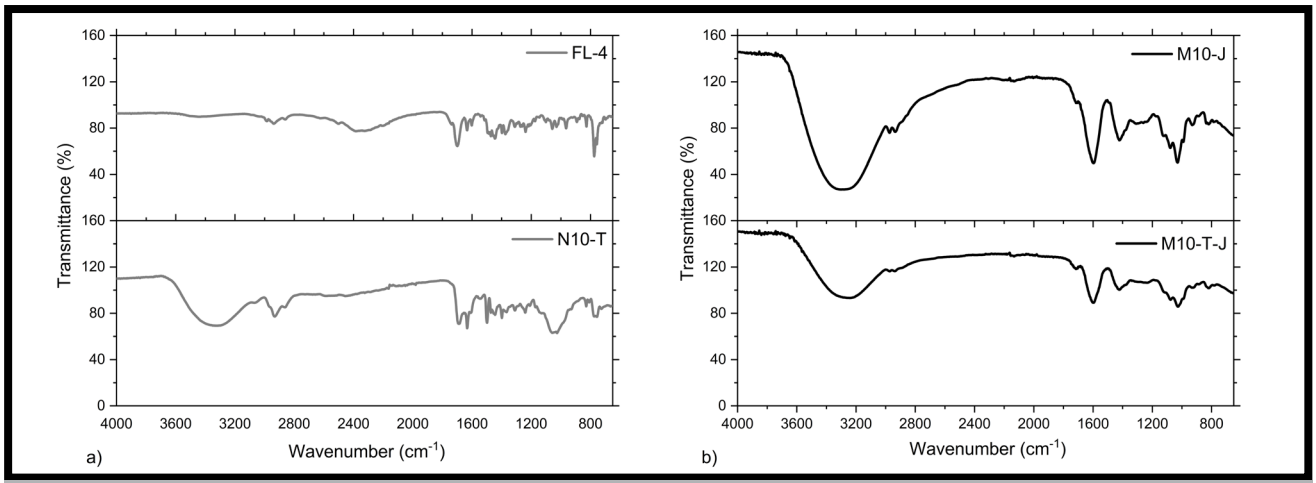

FIG. 4. The FT-IR spectra of the examined compound FL-4, thermosensitive nanocarrier with FL-4 (N10-T) (a) and hydrogel carriers (M10-J, M10-T-J) (b).

In the FT-IR spectra of ionically cross-linked hydrogels (M10-J, M10-T-J), characteristic bands related to ionic interactions in their structure were observed. The band in the range 1550–1650 cm^{-1} is associated with the deformation vibrations of carboxylate groups (COO^-), indicating the presence of ionic bonds formed during ionic cross-linking. Additionally, the band in the range 1400–1450 cm^{-1} corresponds to the symmetric stretching vibrations of carboxylate groups, but their intensity is low, indicating weaker bonds characteristic of ionic cross-linking interactions. The band in the range 2850–3000 cm^{-1}, observed in the M10-J spectra, is due to the presence of compound FL-4 and corresponds to C–H stretching vibrations originating from both aliphatic ($–CH_2$, $–CH_3$) and aromatic (C–HAr) functional groups. In the case of M10-T-J, a very weak peak corresponding to the presence of fananserin derivatives was observed, which may explain the specific behavior of this system in swelling, cross-linking, and active substance release analyses. This result indicates potential interactions between the thermosensitive nanoparticle-FL-4 system and the cross-linking agent, which may significantly influence the properties of the hydrogel.

The sample containing only the thermosensitive nanocarrier with FL-4 (N-T) showed an intense band around 1650 cm^{-1}, which may indicate a high content of bonds characteristic of the polymeric structure (C=O). The broad peak around ~3300 cm^{-1} is due to the vibrations of hydroxyl groups (-OH), and the band in the range 2850–3000 cm^{-1} indicates the presence of the compound FL-4. Additionally, the band at 1050 cm^{-1} can be attributed to stretching vibrations of C-O-C groups, indicating the presence of glycosidic bonds in the thermosensitive nanocarrier structure.

Morphological analysis

Scanning electron microscopy (SEM) is one of the primary tools for assessing the morphology and topography of hydrogel materials, enabling a detailed analysis of the network structure and the distribution of components within the matrix. In the conducted studies, a morphological analysis was performed on two ionically cross-linked hydrogel systems: M10-J and M10-T-J (FIG. 5).

Microscopic observations showed that both systems exhibited irregular shapes, with varying pore sizes and openness. Despite the use of different strategies for incorporating compound FL-4, directly in the case of M10-J and with the use of a thermosensitive nanocarrier in M10-T-J, no significant differences in surface morphology were observed. The structure of the hydrogels in both cases showed comparable degrees of porosity and spatial arrangement. The bright areas visible in the SEM images indicate the presence of the compound FL-4 and its even distribution across the hydrogel matrix surface. These results suggest that the presence of the nanocarrier does not significantly affect the spatial architecture of the hydrogels, and the method of incorporating the compound does not disrupt the integrity of the polymer network at the macro- and microscopic scales.

EDS analysis

The analysis was performed to assess the distribution of the biologically active substance FL-4 on the surface of the hydrogel carriers, with particular attention to the presence of the fluorine atom, which is a unique structural element of compound FL-4 and does not occur in the polymer matrix.

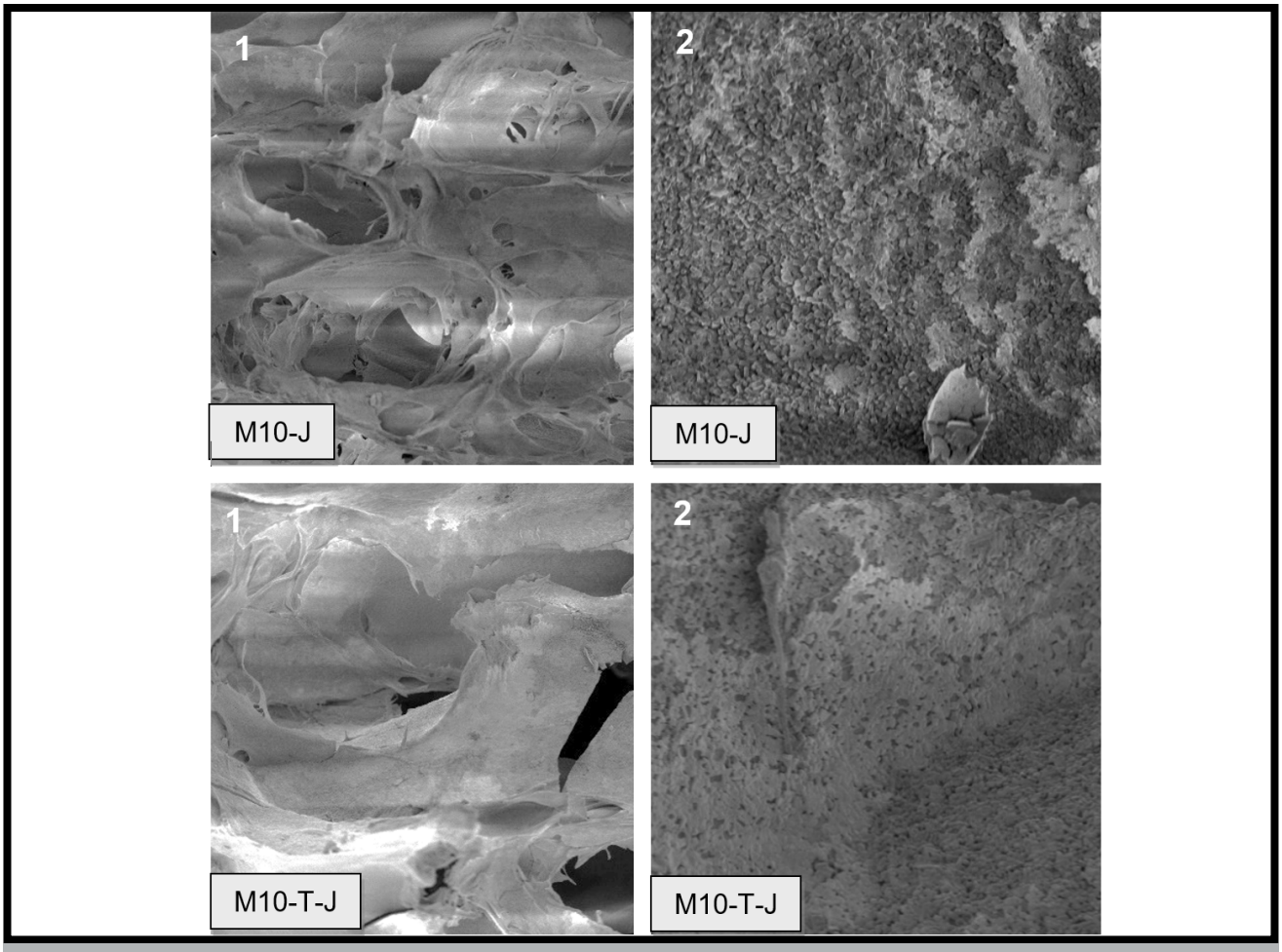

FIG. 5. SEM images of hydrogel carriers: M10-J and M10-T-J at magnifications of 500x (1) and 5000x (2).

The presence of fluorine was confirmed in both M10-J and M10-T-J hydrogels, in amounts of 1.6% and 1.8%, respectively (TABLE 2). The slightly higher fluorine content in the M10-T-J sample may be due to the presence of the thermosensitive nanocarrier, which potentially modifies the distribution of FL-4, promoting its surface exposure. The mapping results presented in FIG. 6 further illustrate the distribution of the fluorine atom on the surface of the examined hydrogels.

In addition to the fluorine atom, the analysis revealed the presence of carbon, oxygen, and nitrogen atoms (FIG. 6) in the tested samples. The M10-J variant showed a higher oxygen content, which may indicate greater exposure of hydrophilic groups on the hydrogel surface.

TABLE 2. Elemental composition [%] on the surface of the examined hydrogel carriers.

Elemental Composition [%]	M10-J	M10-T-J
C	26.6	33.5
N	5.2	5.3
O	66.6	59.4
F	1.6	1.8

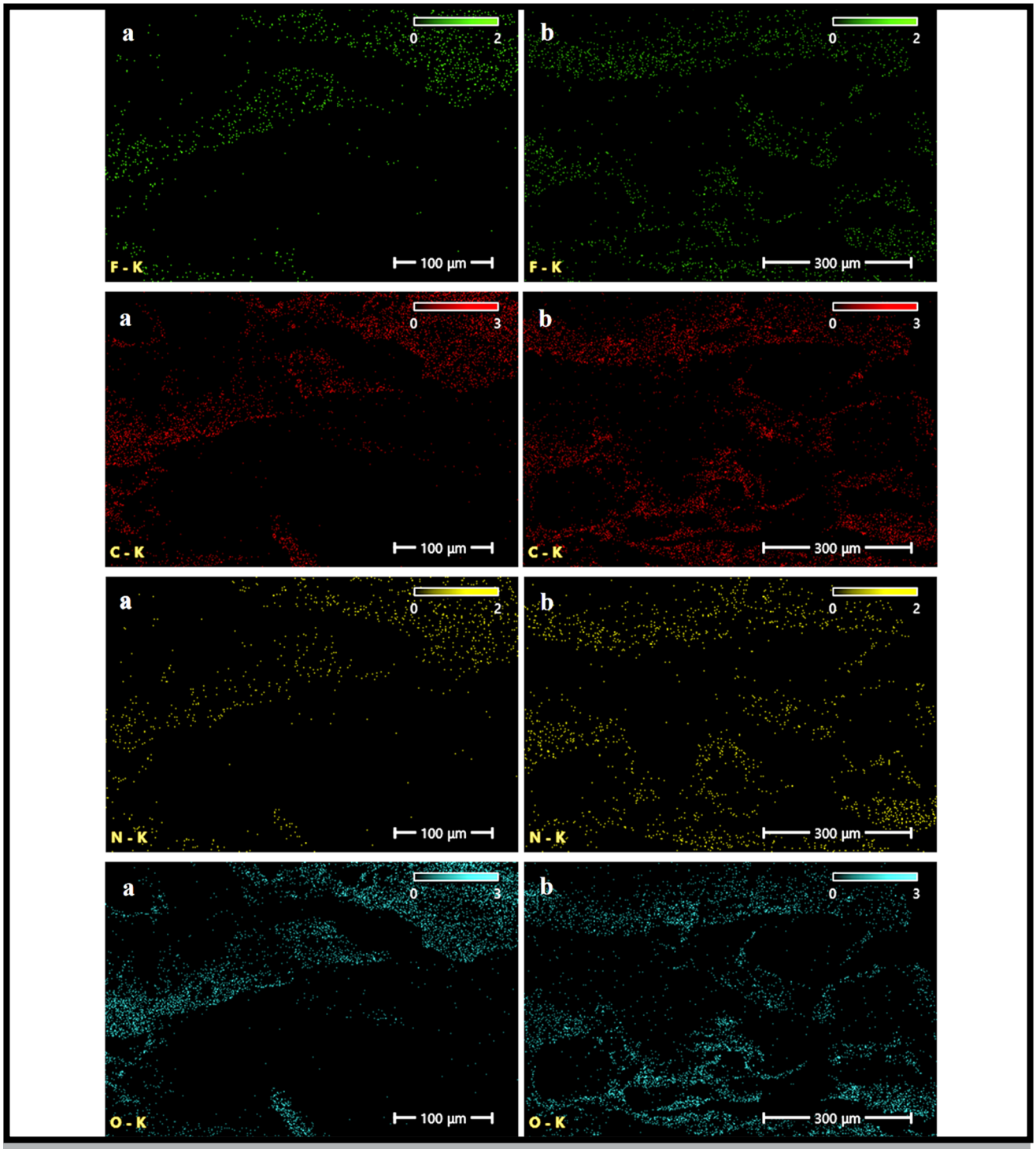

FIG. 6. Fluor (F-K), carbon (C-K), nitrogen (N-K), and oxygen (O-K) mapping on the surface of the examined hydrogel carriers: (a) M10-J and (b) M10-T-J.

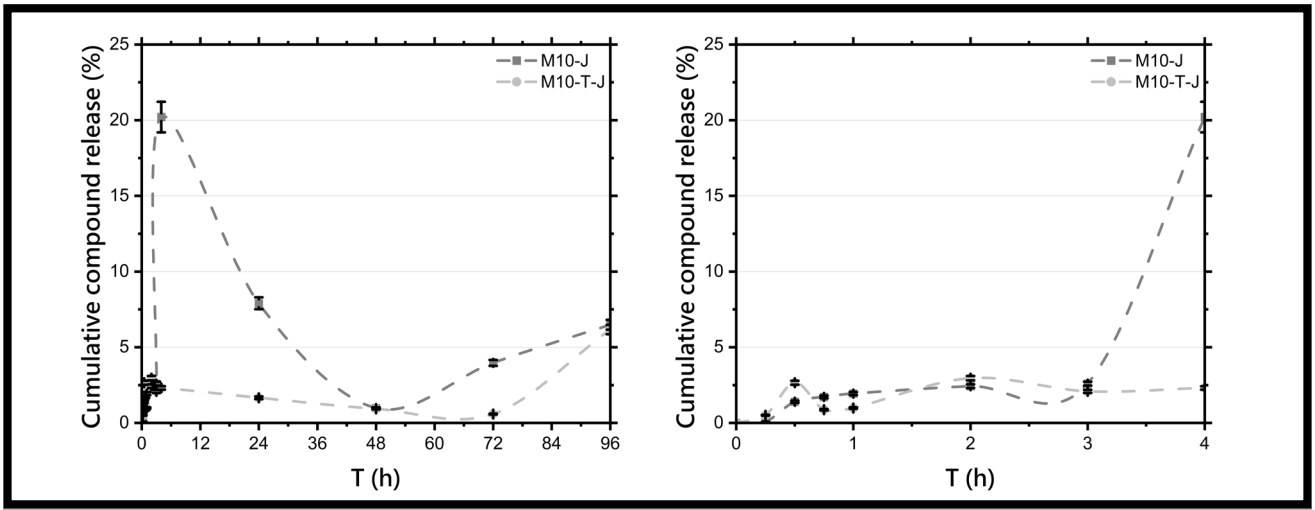

FIG. 7. Comparison of the release profiles of compound FL-4 from hydrogel carriers: FL-4 incorporated directly (M10-J) and systems containing the thermosensitive nanocarrier–compound FL-4 (M10-T-J); the studies were conducted at pH = 7.4 and T = 37°C.

Release profiles of compound FL-4 from the obtained hydrogel carriers

Based on the conducted studies, it can be concluded that the release profile of compound FL-4 from the obtained hydrogel carriers shows significant differences due to the presence of the thermosensitive nanocarrier, as shown in FIG. 7.

In the case of the M10-T-J matrix, only minimal release of compound FL-4 was observed. This effect can be attributed to strong interactions between the nanocarrier and the cross-linking agent, which lead to the closure of the matrix structure, thereby limiting the diffusion of the active substance. This result suggests the formation of a low-porosity structure that effectively restricts drug release from the hydrogel.

Moreover, the poor solubility of FL-4 in aqueous environments, resulting from its strongly hydrophobic nature, may be an additional factor significantly limiting its release. Hydrophobic compounds typically exhibit limited interaction with hydrophilic matrices, such as alginate-based hydrogels, often resulting in low mobility within the network and the tendency to aggregate or become trapped in the inner regions of the polymer matrix [36,37]. These characteristics hinder effective diffusion into the surrounding medium, especially in systems where polymer density or cross-linking is increased, such as in the presence of nanocarriers and divalent ions [38].

The M10-J matrix, in contrast, showed a rapid increase in release within the first 4 h. This phenomenon can be explained by weaker ionic cross-linking, which is consistent with literature findings regarding ionically cross-linked hydrogels [37]. Rapid initial release may suggest that the compound FL-4 is located mainly on the surface of the matrix and is weakly bound to its structure. Additionally, the absence of the thermoresponsive nanocarrier may result in a more open, loosely cross-linked network, which facilitates faster diffusion of the active substance. SEM-EDS analysis, showing the presence of fluorine atoms on the matrix surface, supports this hypothesis by confirming the localization of FL-4 near or at the matrix boundary.

Overall, the low release efficiency from the M10-T-J system likely results from a combination of factors: the hydrophobicity and limited aqueous solubility of FL-4, stronger matrix cross-linking due to interactions with the nanocarrier and Ca^{2+} ions, and potentially deeper entrapment of the drug within a compact polymer network.

Conclusions

Based on the preliminary studies, the optimal concentration of compound FL-4 (10 mg) was selected, ensuring system stability and enabling the development of two types of hydrogel carriers. The first, M10-J, contained FL-4 directly incorporated into the system, while the second, M10-T-J, was a system combining a thermosensitive nanocarrier with FL-4, both of which were ionically cross-linked. The obtained results showed that the presence of the nanocarrier significantly influenced the physicochemical properties of the materials. The increased swelling in M10-T-J samples suggests the formation of weaker, as well as less compact, network structures. Additionally, degradation studies suggest that the degradation process can occur faster in the case of M10-T-J hydrogel, which results also from looser polymer networks. The chemical structure of the biomaterials was confirmed using FT-IR analysis, which indicated the presence of characteristic functional groups associated with sodium alginate, *Aloe vera*, and FL-4. Notably, bands in the range of 2850–3000 cm^{-1} corresponded to C–H stretching vibrations from aromatic and aliphatic groups within the FL-4 molecule, supporting the effective incorporation of the compound into the hydrogel matrix. SEM morphology assessment showed no significant changes in the structure, despite the introduction of the nanocarrier system. However, the release studies showed that the M10-J system releases FL-4 faster as compared to M10-T-J, suggesting that direct incorporation of the active substance may be more effective in applications requiring rapid action. Further studies are needed to fully understand the degradation mechanisms and release of active substances from these advanced carrier systems, as well as additional research in microbiology and cytotoxicity.

Acknowledgements

The work was co-financed by the FutureLab PK program (edition 22/23): project "Programming Excellence – PK XXI 2.0, the development program of the Cracow University of Technology for the years 2018-22" funded by the European Social Fund, Agreement No. POWR.03.05.00-00-z224/17; project "THE PATH TO EXCELLENCE – a comprehensive support program for universities" implemented under the Operational Program Knowledge Education Development 2014-2020, co-financed by the European Social Fund, Agreement No. POWR.03.05.00-00-Z214/18.

References

[1] Y. Zhao, et al.: Cryptococcus neoformans, a global threat to human health. Infect. Dis. Poverty 12(1) (2023), doi: 10.1186/s40249-023-01073-4.
[2] K. Nielsen, et al.: Cryptococcus neoformans α strains preferentially disseminate to the central nervous system during coinfection. Infect. Immun. 73(8) (2005) 4922–4933, doi: 10.1128/IAI.73.8.4922-4933.2005.
[3] WHO, WHO fungal priority pathogens list to guide research, development and public health action (2022), https://www.who.int/publications/i/item/9789240060241
[4] E. Gaviria Morales, et al.: Primary Cutaneous Cryptococcosis due to Cryptococcus neoformans in an Immunocompetent Host Treated with Itraconazole and Drainage: Case Report and Review of the Literature. Case Rep. Dermatol. 13(1) (2021) 89–97, doi: 10.1159/000512289.
[5] E.K. Maziarz, J.R. Perfect: Cryptococcosis. Infect. Dis. Clin. North Am. 30(1) (2016) 179–206, doi: 10.1016/j.idc.2015.10.006.
[6] M.A. Nowak, et al: Cutaneous cryptococcosis: an underlying immunosuppression? Clinical manifestations, pathogenesis, diagnostic examinations and treatment. Postep. Dermatologii i Alergol. 37(2) (2020) 154–158, doi: 10.5114/ada.2020.94833.
[7] P. Zaręba, et al.: Design, synthesis and molecular modelling of new bulky Fananserin derivatives with altered pharmacological profile as potential antidepressants. Bioorganic Med. Chem. 27(15) (2019) 3396–3407, doi: 10.1016/j.bmc.2019.06.028.
[8] H.S. Rane, et al.: Candida albicans VMA3 is necessary for V-ATPase assembly and function and contributes to secretion and filamentation. Eukaryot. Cell 12(10) (2013) 1369–1382, doi: 10.1128/EC.00118-13.
[9] A. Kai, et al.: Diarrheagenic Escherichia coli. Nippon rinsho. Japanese J. Clin. Med. 68 Suppl. 6, (2010) 203–207.
[10] M. Bialik, et al.: Biodegradable synthetic polyesters in the technology of controlled dosage forms of antihypertensive drugs–the overview. Expert Opin. Drug Deliv. 16(9) (2019) 953–967, doi: 10.1080/17425247.2019.1651716.
[11] N. Kamaly, et al.: Degradable controlled-release polymers and polymeric nanoparticles: Mechanisms of controlling drug release. Chem. Rev., 116(4) (2016) 2602–2663, doi: 10.1021/acs.chemrev.5b00346.
[12] P. Trucillo: Drug Carriers: Classification, Administration, Release Profiles, and Industrial Approach. Processes 9(470) (2021) 1–18.
[13] M. Wrzecionek, et al.: Materiały hydrożelowe i ich zastosowanie w medycynie. In: Wybrane rozwiązania technologiczne w medycynie. Wydawnictwo Naukowe TYGIEL sp. z o.o. (2018) 79–96.
[14] Q. Chai, Y. Jiao, X. Yu: Hydrogels for biomedical applications: Their characteristics and the mechanisms behind them. Gels 3(1) (2017), doi: 10.3390/gels3010006.
[15] B. Farasati Far, et al.: Hydrogel Encapsulation Techniques and Its Clinical Applications in Drug Delivery and Regenerative Medicine: A Systematic Review. ACS Omega 9(27) (2024) 29139–29158, doi: 10.1021/acsomega.3c10102.
[16] N. Parvin, et al.: Cutting-Edge Hydrogel Technologies in Tissue Engineering and Biosensing: An Updated Review. Materials (Basel). 17(19) (2024), doi: 10.3390/ma17194792.
[17] M. Verhulsel, et al.: A review of microfabrication and hydrogel engineering for micro-organs on chips. Biomaterials 35(6) (2014) 1816–1832, doi: 10.1016/j.biomaterials.2013.11.021.
[18] S. Lopes, et al.: Ionic- and photo-crosslinked hydrogels. In: Hydrogels for Tissue Engineering and Regenerative Medicine, Academic Press (2024) 181–198. doi: 10.1016/B978-0-12-823948-3.00036-1.
[19] J. Walczak, et al.: Hydrogels based on ionically and covalently crosslinked alginates. Engineering of Biomaterials 132 (2015) 17-23.
[20] J.M. Calderón Moreno, et al.: Eco-Friendly Conductive Hydrogels: Towards Green Wearable Electronics. Gels 11(4) (2025) 220, https://doi.org/10.3390/gels11040220.
[21] Y. Wang, et al.: Progress in Research on Metal Ion Cross-linking Alginate-Based Gels. Gels 11(1) (2025) 16, doi: 10.3390/gels11010016.
[22] K. Bialik-Wąs, et al.: Impact of the Type of Cross-linking Agents on the Properties of Modified Sodium Alginate/Poly(vinyl Alcohol) Hydrogels. Molecules 26(8) (2021) 2381.
[23] K. Draget, et al.: Alginates form algae. In: Steinbuchel A.; Rhee S.K.; (eds) Polysaccharides and polyamides in the food industry. Properties, production, and patents. Wiley; Weinheim, 1–30, 2005, http://onlinelibrary.wiley.com/doi/10.1002/3527600035.bpol6008/full
[24] A. Hamerska-Dudra: Termoczułe polimery usieciowane – synteza i wybrane właściwości. PhD Thesis, Wrocław University of Science and Technology (2007).
[25] X. Li, X. Su: Multifunctional smart hydrogels: Potential in tissue engineering and cancer therapy. J. Mater. Chem. B 6(29) (2018) 4714–4730, doi: 10.1039/c8tb01078a.
[26] M. Sponchioni, et al.: Thermo-responsive polymers: Applications of smart materials in drug delivery and tissue engineering. Mater. Sci. Eng. C 102 (2019), 589–605, doi: 10.1016/j.msec.2019.04.069.
[27] Y. Qu, et al.: A biodegradable thermo-responsive hybrid hydrogel: Therapeutic applications in preventing the post-operative recurrence of breast cancer. NPG Asia Mater. 7(8) (2015) e207-10, doi: 10.1038/am.2015.83.
[28] S. Chatterjee, et al.: Thermoresponsive hydrogels and their biomedical applications: Special insight into their applications in textile based transdermal therapy. Polymers (Basel) 10(5) (2018), doi: 10.3390/polym10050480.
[29] M. Ward: Thermoresponsive Polymers for Biomedical Applications. Polymers (Basel) 3 (2011), doi: 10.3390/polym3031215.
[30] K. Bialik-Wąs, et al.: Bio-Hybrid Hydrogels Incorporated into a System of Salicylic Acid-pH/Thermosensitive Nanocarriers Intended for Cutaneous Wound-Healing Processes. Pharmaceutics 14(4) (2022), doi: 10.3390/pharmaceutics14040773.
[31] S. Chen, et al.: Reaction mechanisms of n-isopropylacrylamide soap-free emulsion polymerization based on two different initiators. J. Macromol. Sci. Part A Pure Appl. Chem. 51(5) (2014) 447–455, doi: 10.1080/10601325.2014.893144.
[32] X. Yan, R.A. Gemeinhart: Cisplatin delivery from poly(acrylic acid-co-methyl methacrylate) microparticles. J. Control. Release 106(1–2) (2005) 198–208, doi: 10.1016/j.jconrel.2005.05.005.
[33] K. Bialik-Wąs, et al.: Poly(acrylic acid-co-methyl methacrylate)/metronidazole systems: Synthesis and complexation. Acta Biochim. Pol. 60(4) (2013) 835–838, doi: 10.18388/abp.2013_2068.
[34] K. Bialik-Wąs, et al.: Sposób Wprowadzania Hydrofobowych Leczniczych Substancji Czynnych, Tworzących Układu z Termoczułym Nanonośnikiem, do Hydrofilowej Matrycy Opatrunku Hydrożelowego. Zgłoszenie patentowe nr P.439845, 15 grudnia 2021 r.
[35] M.G. Sosa-Herrera, et al.: Effect of added calcium chloride on the physicochemical and rheological properties of aqueous mixtures of sodium caseinate/sodium alginate and respective oil-in-water emulsions. Food Hydrocoll. 29(1) (2012) 175–184, doi: 10.1016/j.foodhyd.2012.02.017.
[36] K.Y. Lee, D.J. Mooney: Hydrogels for tissue engineering. Chem. Rev. 101(7) (2001) 1869–1879, doi: 10.1021/cr000108x.
[37] N.A. Peppas, et al.: Hydrogels in pharmaceutical formulations. Eur. J. Pharm. Biopharm. 50(1) (2000) 27–46, doi: 10.1016/S0939-6411(00)00090-4.
[38] J.S. Boateng, et al.: Wound healing dressings and drug delivery systems: A review. J. Pharm. Sci. 97(8) (2008) 2892–2923, doi: 10.1002/jps.21210.